Reactor Intensification on Glycerol-to-Acrylic Acid Conversion: A Modelling Study

Prashant Pawanipagar[1], Kamran Ghasemzadeh[1], Carmine D'Agostino[1,2], Vincenzo Spallina[1]*

[1]Department of Chemical Engineering, University of Manchester, M13 9PL Manchester, UK

[2]Dipartimento di Ingegneria Civile, Chimica, Ambientale e dei Materiali (DICAM), Alma Mater Studiorum – Università di Bologna, Via Terracini, 28, 40131 Bologna, Italy.

* Corresponding author: vincenzo.spallina@manchester.ac.uk

A. Dehydration process

A.1. Numerical procedure and mesh independency

The simulations were performed for dehydration reaction at operating conditions of 1 bar, 613 K, GHSV of 4000 hr^{-1}, and a glycerol mass fraction of 0.1 (refer to figure 1). The results indicate beyond a mesh number of 10972, glycerol conversion and acrolein yield changes are less than 0.13%. Consequently, all subsequent simulations were performed using this grid refinement for glycerol dehydration.

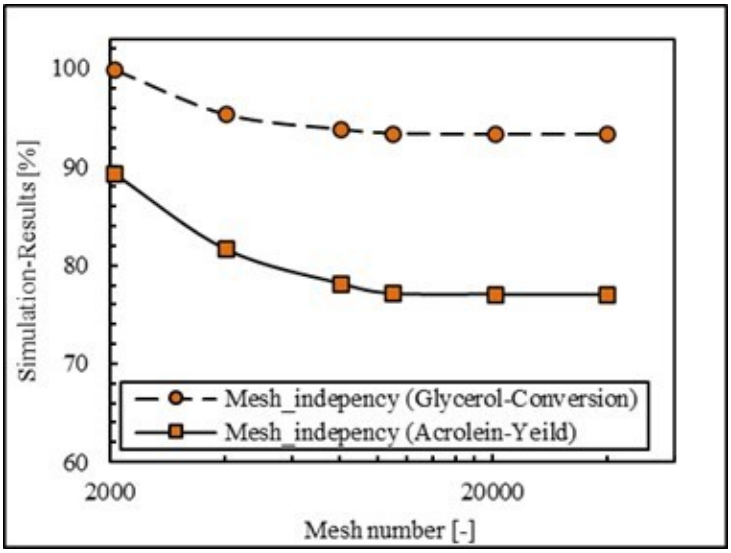

Figure 1: Effect of mesh numbers on calculated glycerol conversion and acrolein yield by CFD model for the case of the PBR (at a reaction pressure of 1 bar, reaction temperature of 613 K, GHSV of 4000 hr-1 and glycerol mass fraction of 0.1).

A.2. CFD model validation

A comparison between numerical results and experimental data for dehydration reveals that the relative error ranges between 1 and 3%. For example, in figure 2, at a low temperature (553 K), the glycerol conversion and the acrolein yield by CFD simulation match the experimental point (with < 1% error).

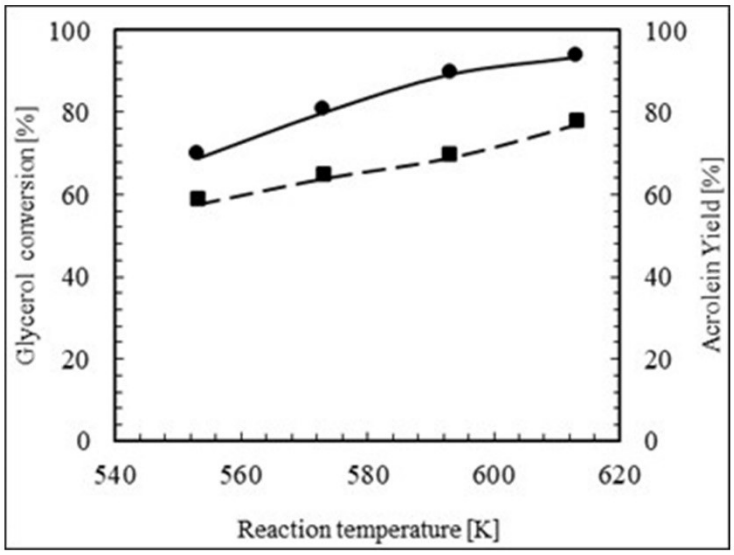

Figure 2: Comparison of glycerol conversion (straight line) and acrolein yield (dashed line) with experimental data provided by literature.

A.3. Experimental design process

In case of dehydration, the model evaluates the combined effects of input variable factors to determine the optimal output. The CFD results were utilized as a reliable data source for training the response surface and subsequently employed in the optimization analysis.

Table 1: Coded levels of three independent variables and Box Behnken design matrix

Run N.	A: Reaction temperature (K)	B: GHSV (hr^{-1}))	C: $C_3H_8O_3$ mass fraction in H_2O mixture (-)
1	543	8250	0.1
2	543	8250	0.5
3	543	1500	0.3
4	583	15000	0.5
5	623	15000	0.3
6	583	8250	0.3
7	543	15000	0.3
8	583	8250	0.3
9	583	1500	0.5
10	623	8250	0.5

11	583	15000	0.1
12	583	1500	0.1
13	583	8250	0.3
14	623	1500	0.3
15	623	8250	0.1

In this analysis, the RSM approach employed a second-order polynomial model for acrolein selectivity and a linear model for acrolein yield and glycerol conversion. These models were utilized to explore the relationship between the response variables and input factors, as outlined below [38]:

$$Re = \beta_0 + \beta_1 A + \beta_2 B + \beta_3 C + \beta_{11} A^2 + \beta_{22} B^2 + \beta_{33} C^2 + \beta_{12} AB + \beta_{13} AC + \beta_{23} BC \quad \text{(Eq.28)}$$

$$Re = \beta_0 + \beta_1 A + \beta_2 B + \beta_3 C \quad \text{(Eq.29)}$$

Where Re is the response factor (glycerol conversion, acrolein yield and acrolein selectivity), A, B, and C are independent input variables (A: Reaction temperature, B: GHSV and C: Glycerol mass fraction), β_0 is the constant coefficient, $\beta_{0\text{-}3}$, $\beta_{12,13,23}$ and $\beta_{11,22,33}$ are interaction coefficients of linear, the second-order and quadratic terms, respectively.

A.4. Statistical analysis

Using the CFD simulation runs, the three-level Box-Behnken method was employed to prioritize the selected input parameters for optimizing acrolein, acrylic acid production and glycerol consumption. As per the statistical interpretation, the design matrix is presented in table 2, which includes the predicted response value of acrolein and acrylic acid selectivity. The linear regression equations and ANOVA tables were generated for the acrolein yield and glycerol conversion cases, and acrylic acid selectivity. Numerical experiments, implemented as CFD runs, were conducted according to the designated experimental design plan (refer to table 1). The quadratic regression equation for acrolein selectivity in terms of factor-coded values is expressed by Eq. 30:

$$Re = 86.43 - 1.0625A + 5.75B - 1.0375C + 0.433333A^2 - 5.6 \cdot 0.75AC - 0.975BC \quad \text{(Eq.30)}$$

However, as mentioned before, a linear regression equation for glycerol conversion and acrolein yield could be suggested. The validated CFD-RSM model provides a comprehensive representation of the effects of each input parameter and their interactions with the response factors, offering a clear visualization of the relationship between the variables.

Table 2: The ANOVA output for response surface quadratic model of acrolein selectivity

Response	Model terms	Sum of squares	Free degree	Mean Square	F-value	P-Value (significant)
Acrolein selectivity (%)	Model Eq.28	416.10	9	46.23	532.44	< 0.0001
	A: Temperature	9.03	1	9.03	104.01	0.0002
	B: GHSV	264.50	1	264.50	3046.07	< 0.0001
	C: Glycerol Mass fraction	8.61	1	8.61	99.17	0.0002
	AB	5.52	1	5.52	63.60	0.0005
	AC	2.25	1	2.25	25.91	0.0038
	BC	3.80	1	3.80	43.79	0.0012
	A^2	0.6933	1	0.6933	7.98	0.0369
	B^2	117.52	1	117.52	1353.40	< 0.0001
	C^2	4.60	1	4.60	53.02	0.0008
R^2=0.9991	Adjusted R^2=0.9971			Adequate precision: 63.8505		

A negative sign in front of the terms in the CFD-RSM model indicates an antagonistic effect, suggesting that the corresponding input factor negatively impacts the response values. Conversely, a positive sign signifies a synergistic effect, indicating that the input factor positively influences the response values. The statistical analysis of the CFD-RSM model quality was conducted using ANOVA, and the results are presented in table 2. The accuracy of

the second-order quadratic regression in the developed model was verified at a 95% confidence level based on the obtained F-value (7.98, 3046.07) and the p-value (<0.05). These results confirm that the model adequately represents acrolein production within the studied range of input variables.

The ANOVA outputs demonstrate a strong correlation between the input variables and the response factors, as evidenced by the coefficient of determination R^2 of 0.9991. This high value indicates a compatible relationship between the model and the observed data. Additionally, the value of R^2_{adj} (0.9971) suggests that less than 1% of the variation cannot be explained by the model. The adequate precision of 63.85 indicates that the developed model provides a sufficient signal-to-noise ratio, allowing for reliable navigation within the design space. Moreover, a ratio value exceeding 4 is desirable, confirming the model's effectiveness.

A.5. Effect of GSHV

The effect of GSHV on key reaction indicators are also presented in figure 3

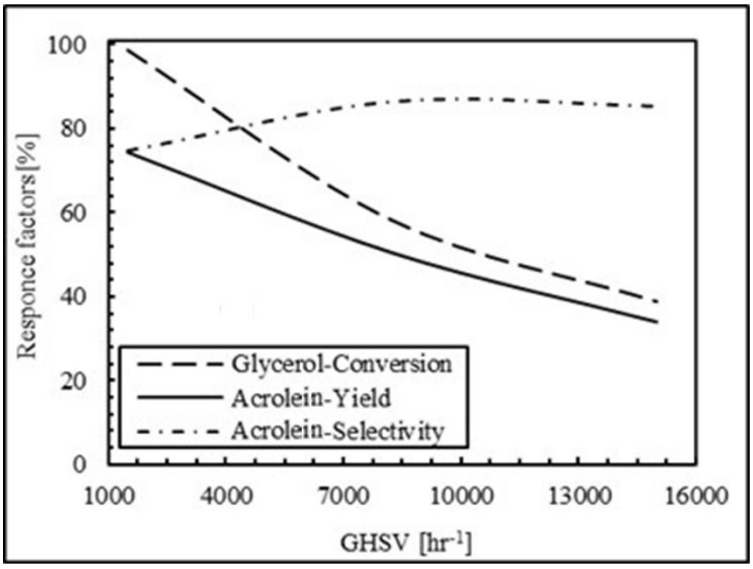

Figure 3: Glycerol conversion, acrolein yield, and acrolein selectivity versus GHSV (at 584 K, 1 bar reaction pressure, and glycerol mass fraction of 0.3)

A.6. Component and velocity distribution

As a further comparative study of glycerol dehydration for acrolein production in the PBR, SMPBR, and MBPR configurations, the acrolein and glycerol mole fraction axial distributions are shown in figure 4

Figure 4: Mole fraction (-) contours achieved by CFD simulations for acrolein (left side) and glycerol (right side); (a) in the PBR configuration, (b) in the SMPBR configuration, and (c) in the MBPR configuration

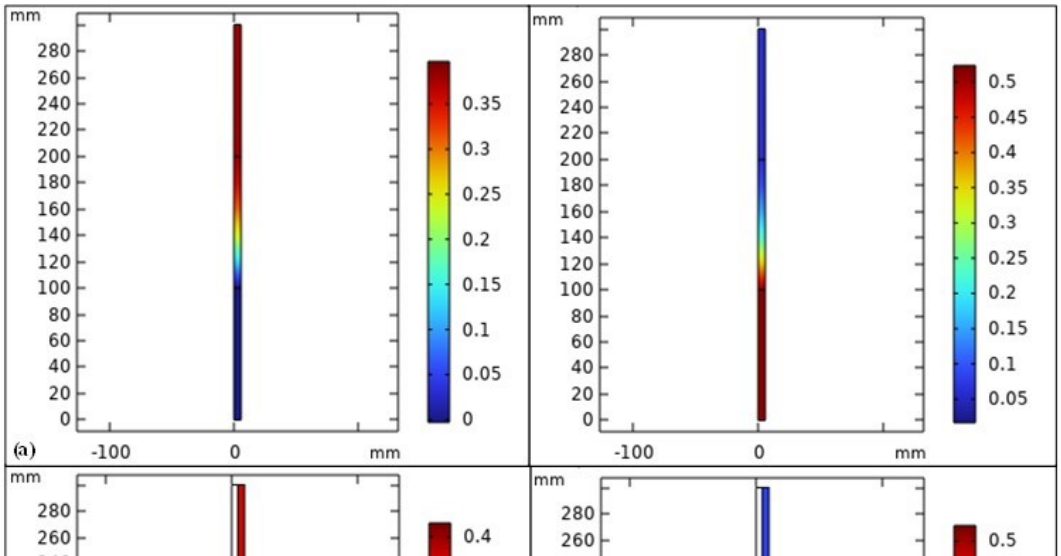

B. Oxidation process

B.1. Numerical procedure and mesh independency

In case of oxidation, the simulations were specifically carried out for the PBR configuration during the acrolein oxidation process, operating at 1 bar pressure, 613 K temperature, a GHSV of 2000 h^{-1}, and an oxygen/acrolein molar ratio of 2. These simulations outcomes focus on parameters such as acrolein conversion and acrylic acid yield, presented in figure 5.

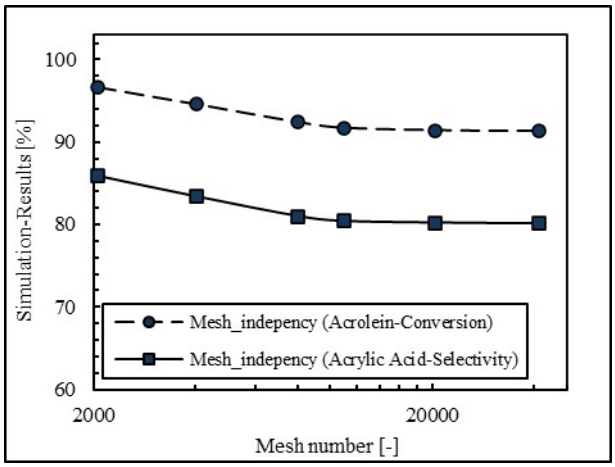

Figure 5: Effect of mesh numbers on calculated acrolein conversion and acrylic acid selectivity by CFD model for the case of the PBR (at 1 bar, 613 K, GHSV of 2000 h-1, and Oxygen/Acrolein ratio of 2).

As the graph shows, increasing the mesh number changes the results which indicates that the simulation accuracies are not constant. For 10972 elements, a minimal change in the results (<0.20%) is recorded by increasing further the number of grid points. Therefore, this mesh size has been used for all the subsequent simulations.

B.2. CFD model validation

The comparative analysis of numerical values with the experimental results shows that the error range lies within 1% to 6%.

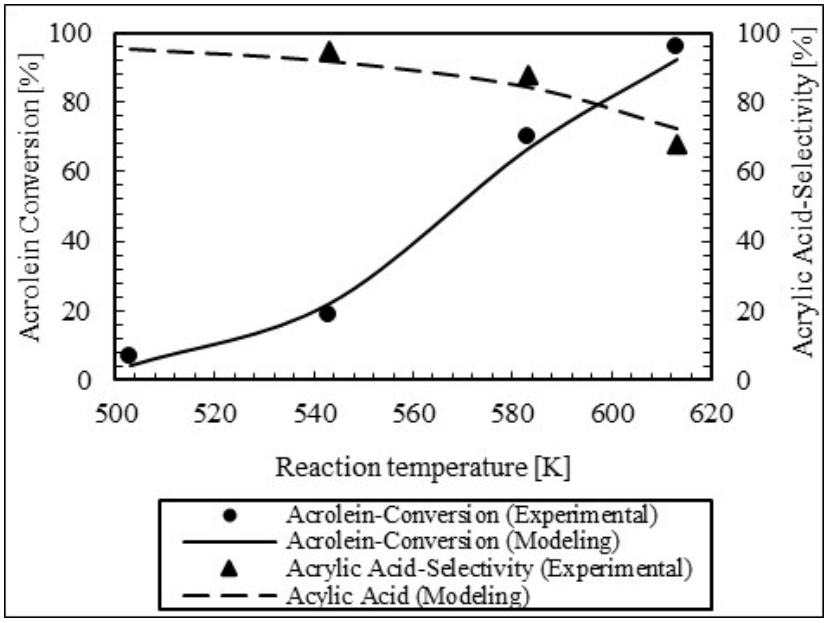

Figure 6: Comparison of the presented CFD results with experimental data provided by literature.

Figure 6 illustrates acrolein conversion and acrylic acid selectivity as a function of reaction temperature. The acrolein consumption and the acrylic acid production rate in terms of concentration contours are described in figure 7.

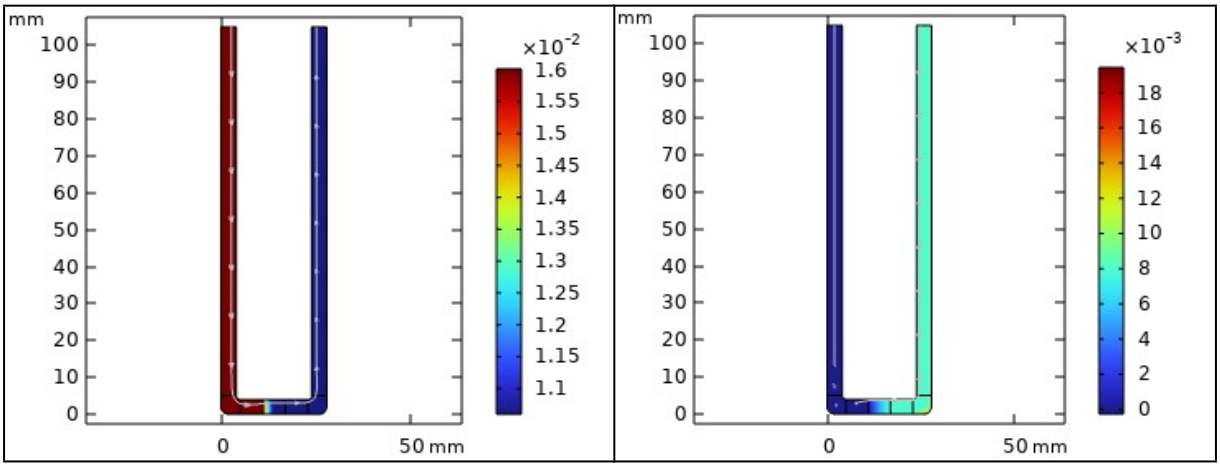

Figure 7: (a) Acrolein concentration distribution and (b) Acrylic acid concentration distribution in experimental setup presented by literature.

B.3. Experimental design process

The independent variables considered in optimization are listed in table 3; this includes reaction temperature, GHSV, and oxygen/acrolein molar feed ratio. These parameters are embraced within the framework of Box-Behnken design, predicting 15 simulation runs considering all possible combinations.

Table 3: Levels of three independent variables and Box Behnken design matrix.

Run No.	Reaction temperature (K)	Gas hour space velocity (GHSV (h^{-1}))	Oxygen/Acrolein molar ratio (-)
1	523	1600	3.25
2	573	16000	0.5
3	573	16000	6
4	573	8800	3.25
5	573	1600	6
6	623	1600	3.25
7	523	16000	3.25
8	523	8800	0.5
9	623	8800	0.5
10	523	8800	6
11	623	8800	6
12	573	1600	0.5
13	573	8800	3.25
14	623	16000	3.25
15	573	8800	3.25

Hence, based on experimental results, CFD-RSM analysis has been implemented to fit the model. The corresponding response factors are acrolein conversion, acrylic acid yield, and selectivity. Moreover, this model also recommended using a quadratic equation model for acrylic acid selectivity, acrylic acid yield, and acrolein conversion. Finally, the model was

applied to examine the complex relationship between parameters and response factors. The equation is listed below, where R represents the response for acrolein conversion, acrylic acid yield, and selectivity.

$$R = \beta_0 + \beta_1 A + \beta_2 B + \beta_3 C + \beta_{11} A^2 + \beta_{22} B^2 + \beta_{33} C^2 + \beta_{12} AB + \beta_{13} AC + \beta_{23} BC \quad \text{(Eq.25)}$$

Here, A, B, and C are independent variables that signify (A- reaction temperature, B- GHSV, C- oxygen/ acrolein molar ratio). β_0 is the constant coefficient, β_{1-3}, $\beta_{11,22,33}$ and $\beta_{12,13,23}$ are interaction coefficients of quadratic model terms.

B.4. Statistical analysis

A three-level-box-Behnken scheme was introduced to estimate the relative significance of the selected influential factor optimizing the process. The objective is to increase acrylic acid production and reduce acrolein consumption using CFD simulation experiments. The complete design matrix, along with the predicted response value of acrylic acid selectivity, is provided as a source for comprehensive statistical analysis. Table 4 encapsulates the quadratic regression equation and ANOVA tables concerning acrolein conversion and acrylic acid selectivity. As per the specified simulation plan (table 3), numerical experiments were performed through CFD. As an example, the quadratic equation for acrylic acid selectivity is expressed as equation 26.

$$Re = 93.9 - 3.68A - 1.46B + 4.81C - 7.62A^2 - 0.8B^2 - 5.25C^2 + 3.53AB - 6. \quad \text{(Eq. 26)}$$

Now, after the validation process, the final version of the CFD-RSM model gives a crystal-clear perception of the impact caused by every influential parameter and their interconnected interaction with the responses. Here, the positive sign indicates a synergistic effect caused by a factor on the response, whereas the negative sign manifests an antagonistic effect. A statistical analysis was conducted to quantify the model standard, and the following outcomes are described in table 4. It can be reported that the 2nd order quadratic model was found to be

correct, with the efficiency of 95%, F-value which is approximately 11.98, and equivalent P-value corresponding to a number less than 0.05. It can be stated that this result confirms the model's adequacy for predicting acrolein production within a specific range of variables applied to the system model.

Table 4: The ANOVA output for response surface quadratic model of acrylic acid selectivity.

Response	Model terms	Sum of squares	Free degree	Mean Square	F-value	P-Value (significant)
Acrylic acid selectivity (%)	Model Eq.26	901.77	9	100.2	11.98	0.007
	A: Temp	108.05	1	108.05	12.92	0.015
	B: GHSV	17.11	1	17.11	2.05	0.212
	C: O_2/ACR ratio	185.28	1	185.28	22.15	0.005
	AB	49.70	1	49.70	5.94	0.059
	AC	165.12	1	165.12	19.74	0.007
	BC	81	1	81	9.68	0.026
	A^2	214.67	1	214.67	25.66	0.004
	B^2	2.36	1	2.36	0.28	0.618
	C^2	101.77	1	101.77	12.17	0.018
R^2=0.96	Adjusted R^2=0.88			Adequate precision: 9.52		

Following the ANOVA results, the coefficient R^2 stands to an absolute value of 0.96, which designates a robust correlation between the independent variables and the responses. The adjusted R^2 value has reached 0.88, implying that the model can account for nearly 96% of the variation, leaving the remaining 4% unexplained. Furthermore, the adequate precision score was 9.52, indicating that the model provides a good signal for navigating a design space.

B.5. Evaluation of component/velocity distribution

Figure 8 schematically depicts the concentration profile, illustrating trends in acrolein consumption distribution, acrylic acid production, and other by-products (CO_2, CO, and H_2O) along the reaction pathway. These profiles are based on operating conditions from run 5 (table 3). Acrylic acid and other by-products are produced along the catalyst bed, while acrolein is consumed primarily during the initial part of the catalyst bed.

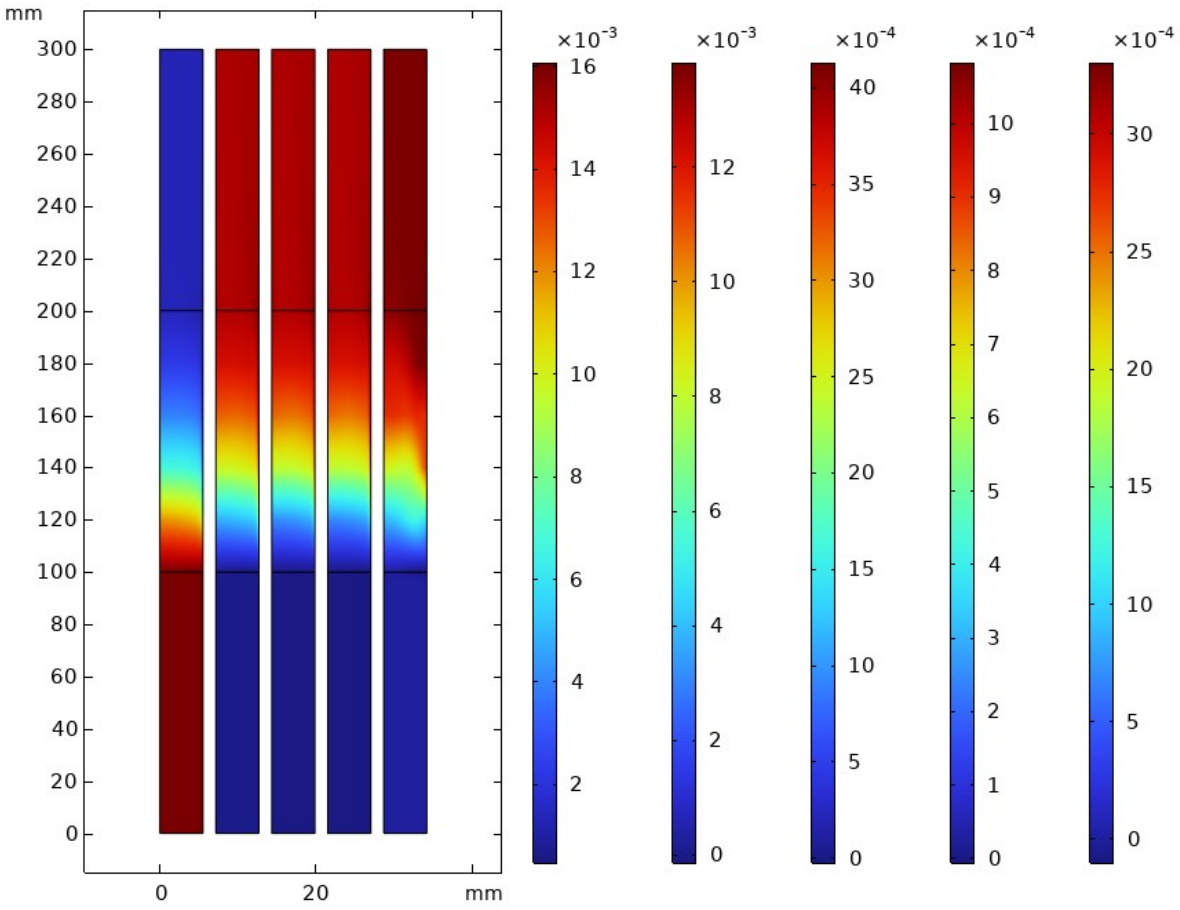

Figure 8: Concentration contours achieved by CFD simulation during acrolein oxidation in the PBR (acrolein, acrylic acid, carbon dioxide, carbon monoxide, and steam in order from left to right)

Figure 9 provides a pictorial representation where different colours indicate pressure and velocity. The pressure drops across the reactor zone's length are around 10 kPa figure 9 (a), as expected due to the catalyst bed. In contrast, the velocity distribution follows a parabolic curve in the inert zone of the packed bed reactor Figure 9(b). The maximum velocity is observed in

the central region of inert streams, both before and after the catalyst bed, which is logical since flow in a cylindrical pipe has a maximum velocity at the centre of the tube.

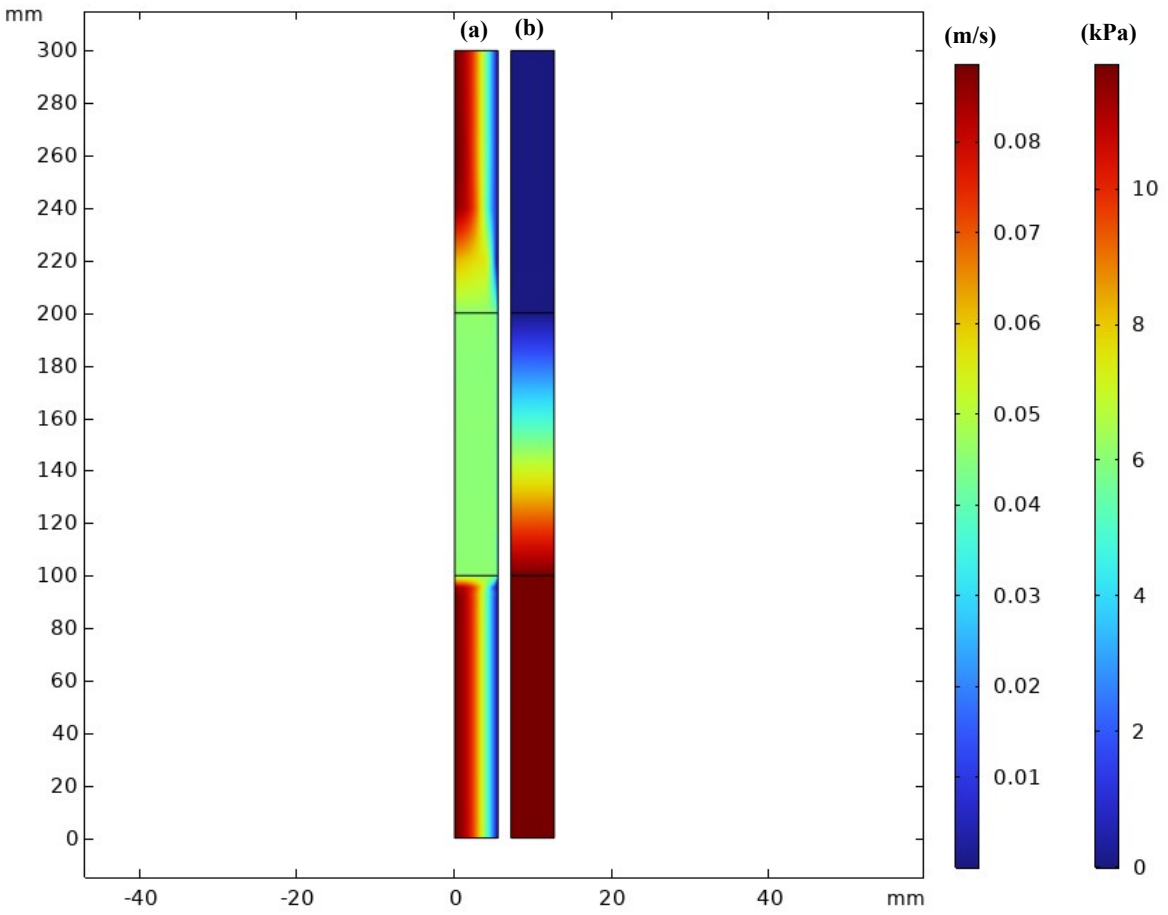

Figure 9: (a) Velocity contour (m/s), (b) Pressure contour (kPa) during acrolein oxidation in the PBR.

Figure 10 shows a 3-D contour indicating the effect of increasing temperature (523 - 623K) and GHSV (1600 - 16000) on acrolein conversion, acrylic acid yield, and acrylic acid selectivity. The acrolein conversion increases with increasing temperature with lower values of GHSV but with increasing GHSV a reduction is observed, and similar behaviour is identified with the acrylic acid yield. However, a different trend was noticed with selectivity. It initially increases reaching maximum value and then reduced w.r.t temperature.

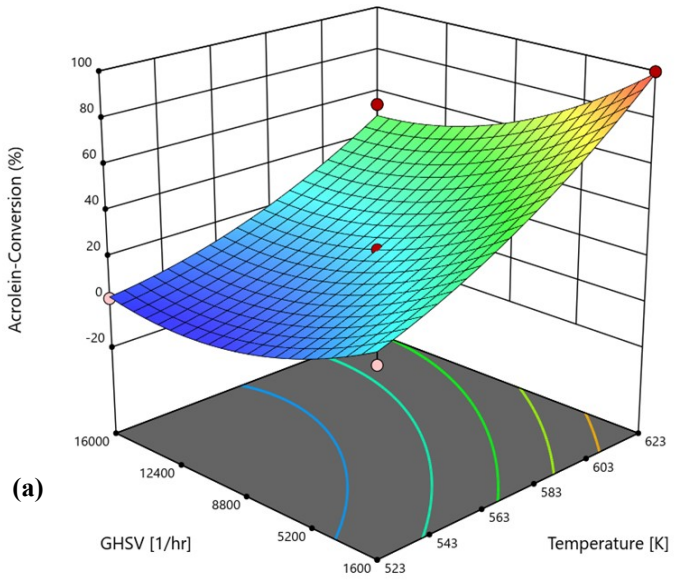
Acrolein-Conversion (%)
100
80
60
40
20
0
-20
16000
12400
8800
5200
1600
GHSV [1/hr]
523
543
563
583
603
623
Temperature [K]

(a)

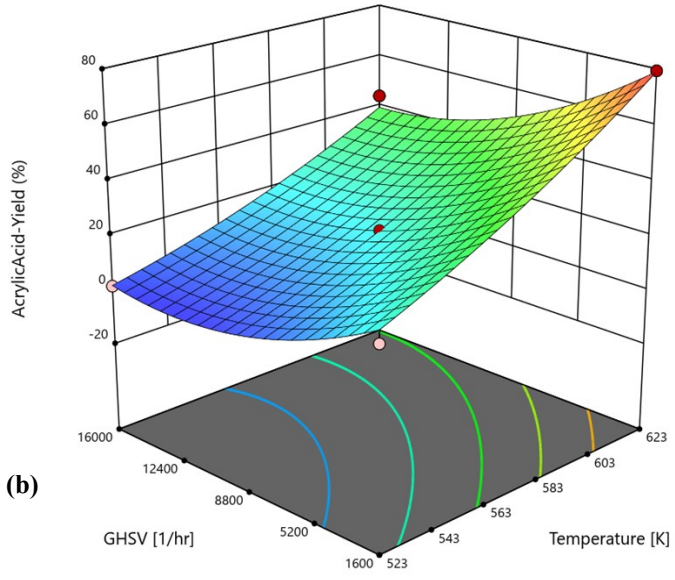
AcrylicAcid-Yield (%)
80
60
40
20
0
-20
16000
12400
8800
5200
1600
GHSV [1/hr]
523
543
563
583
603
623
Temperature [K]

(b)

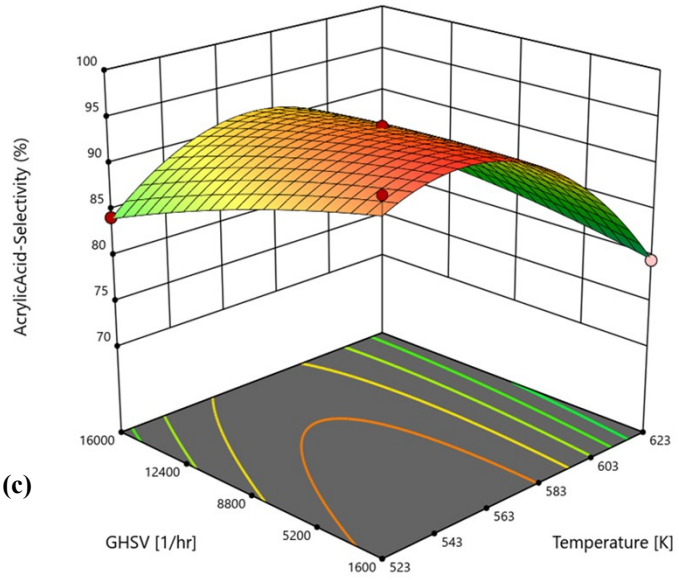
AcrylicAcid-Selectivity (%)
100
95
90
85
80
75
70
16000
12400
8800
5200
1600
GHSV [1/hr]
523
543
563
583
603
623
Temperature [K]

(c)

Figure 10: Glycerol conversion, acrolein yield, and acrolein selectivity versus GHSV (at 584 K, 1 bar reaction pressure, and glycerol mass fraction of 0.3)